JOURNAL OF MATERIALS SCIENCE 30 (1995) 4871–4881

Lockup, chains and the delocalization of damage

B. N. COX
Rockwell Science Center, 1049 Camino Dos Rios, Thousand Oaks, CA 91360, USA

Whether damage is localized or delocalized in a composite, the composite's fracture toughness when localization occurs can be controlled to a much greater extent than hitherto exploited by properly choosing the composite's internal geometry. Delocalization and high toughness are both favoured by building in systematic defects and lock-up mechanisms. Widespread defects make available arbitrarily many sites at which energy may be absorbed by non-linear behaviour. Lock-up mechanisms cause local hardening following local damage, which drives subsequent damage to initiate elsewhere, possibly leading to damage delocalization. In brittle–brittle composites, these mechanisms may be the best hope for achieving toughness values similar to those of alloys. Illustrations are taken from recent research into woven composites with three-dimensional reinforcement and new work on model composites.

1. Introduction

When a material begins to fail under load, irreversible damage may occur more or less uniformly over the entire loaded volume before a localized damage band forms and causes ultimate failure. Representative cases are shown schematically in Fig. 1. This paper addresses the question of how the reinforcement in a composite might be arranged geometrically

1. to activate delocalized rather than localized damage, and
2. to maximize toughness when a localized damage band does form.

The key problem is controlling displacements and stress redistribution around local failure events within the composite to avoid damage propagation driven by stress concentration. The potential of this approach will be illustrated by model materials.

1.1. Ductile materials

Engineering stress–strain curves, $\sigma_e(e)$, for tensile tests of some ductile materials are shown in Fig. 2. Whether global strain can increase uniformly without localization in an unnotched specimen depends on the stability of the system with respect to fluctuations in strain. For a material that conserves volume during deformation, so that the cross-sectional area decreases as strain increases, a positive axial strain fluctuation increases the local *true* stress. Stability requires that this stress increase be less than that implied by the true stress–true strain constitutive relation, $\sigma(\varepsilon)$, for the same fluctuation in strain; or (e.g. [2])

$$\frac{d\sigma}{d\varepsilon} > \sigma \tag{1}$$

For the *engineering* stress and strain, Equation 1 is equivalent to the condition $d\sigma_e/de > 0$. Thus necking will begin in a uniaxial tension bar of mild steel or brass at the peaks in the $\sigma_e(e)$ curves in Fig. 2a. The post-peak tails of the curves in Fig. 2a reflect the development of high levels of plastic strain localized to the necking region.

Polycarbonate and polyethylene (Fig. 2b) are typical of cold drawing polymers. In these materials, the condition Equation 1 is satisfied twice [3]: once at low strain, ε_1, and again at a much higher strain, ε_2 (and higher stress). When the strain, ε_1, is reached in a tensile test, necking will set in at some part of the specimen. However, when the necking material exceeds the true strain, ε_2, it can harden sufficiently that further plastic strain is arrested there and plasticity spreads into neighbouring material instead*. The boundaries of the neck propagate in a self-similar fashion and thus the entire specimen is drawn until it shares, more or less uniformly, a true strain exceeding ε_2. Further loading causes failure. Cold drawing is the origin of the very high engineering strains for the polymers of Fig. 2b. Microscopically, the hardening that stabilizes necking reflects straightening of molecular chains that were initially folded.

For any of the materials represented in Fig. 2, the damage localization leading to ultimate failure commences at the global maximum of the engineering stress–strain curve. The global plastic work, W_p, per unit volume prior to this localization can be

*That Equation 1 should be satisfied twice is a necessary, but not sufficient, condition for cold drawing. Whether the polymer draws depends on how it responds to a complex triaxial stress state when Equation 1 is satisfied for the second time in the first necked region. Such details are beyond the interest of this paper.

0022–2461

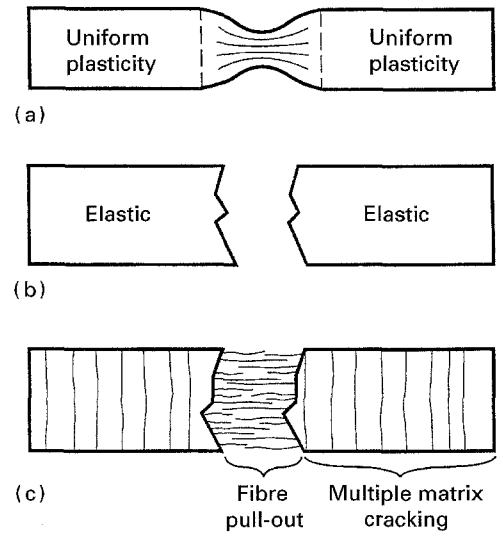

Figure 1 Schematics of uniaxial tensile tests showing global damage and localized damage band: (a) ductile (necking) material, (b) brittle material, and (c) brittle–brittle fibrous composite.

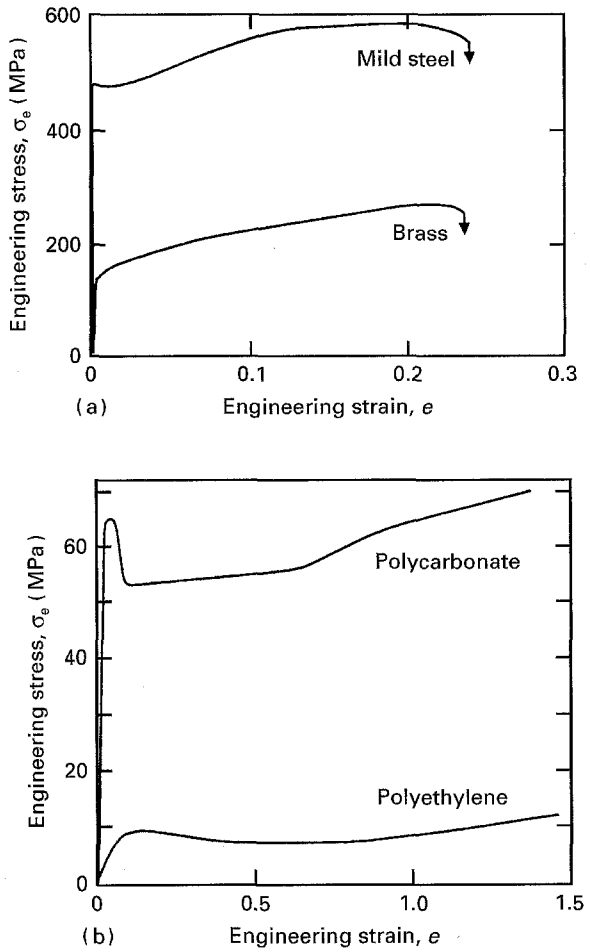

Figure 2 Engineering stress–strain curves for some ductile materials in uniaxial tension (taken from [1]): (a) metal alloys, and (b) polymers.

calculated from the true stress and strain

$$W_p = \int_0^{\varepsilon_2 - \sigma_2/E} \sigma d\varepsilon_p \qquad (2)$$

where ε_2 is the true strain at the global maximum in $\sigma_e(e)$; $\sigma_2 \equiv \sigma(\varepsilon_2)$; and $\varepsilon_p \equiv \varepsilon - \sigma(\varepsilon)/E$ is the plastic strain. Representative values are listed in Table I. For ductile materials, they are 10–100 MJ m^{-3}.

Following the localization that leads to ultimate failure, further work must be expended to separate the specimen in two. This work should be independent of specimen length; it is a work per unit area.

1.2. Brittle materials

In a material as brittle as monolithic glass, there is no measurable global plastic work, W_p, expended prior to damage localization. Failure occurs by the propagation of a crack from some possibly microscopic flaw, while the material away from the crack tip generally remains elastic.

In a brittle material reinforced by strong, continuous brittle fibres, global damage can occur via multiple matrix cracking (Fig. 1c) [4]. The stress–strain curve for a uniaxial tension test is typified by Fig. 3. Global plastic work, which is uniform over gauge lengths much greater than the crack spacing, is absorbed by friction when the matrix and fibres slide relative to one another near each matrix crack. Damage localization occurs when a critical number of fibres fail, and ultimate failure ensues with little further increase in applied strain. The plastic strain is therefore limited by the failure strain of the fibres. The global plastic work remains very modest. Table I shows values estimated from representative published stress–strain curves [5]: $W_p \sim 1$ kJ M^{-3}. These modest values are the highest yet attained for composites of ceramic constituents.

Global plastic work occurs by a similar mechanism of multiple cracking in unidirectional and 0/90° polymer composites. Representative values of W_p, which can be deduced from stress–strain curves quite like those of Fig. 3 [6], are similar to those for ceramic composites.

1.3. Work of fracture

When ultimate failure occurs by damage localized in a band, its energetics can be summarized by considering the tractions, p, developed across the localized damage band as a function of the displacement discontinuity, $2u$, the band produces (Fig. 4). The displacement discontinuity, $2u$, is defined by

$$2u = \Delta - \varepsilon d \qquad (3)$$

where Δ is the total displacement observed along a gauge of length d that wholly contains the damage band and ε is the far field strain.

Many forms have been conjectured or measured for the relation $p(u)$. Dugdale proposed a uniform function, p = constant, to describe localized yielding in a notched ductile metal in plane stress [7]. Tension–softening relations are common in modelling concrete (e.g. [8, 9]) or polymers [10]. In some systems, e.g. brittle matrix composites reinforced by fibres or ductile metal inclusions, $p(u)$ rises to a peak corresponding to bridging ligament failure before falling back to zero at large displacements (Fig. 5). If there

TABLE I Some ranges of material properties related to ductility

	W_p ($J\,m^{-3}$)	J_c ($J\,m^{-2}$)	σ_c (MPa)	l_{ch} (mm)
Ductile metal	$40–100 \times 10^6$	$< 200 \times 10^3$	200–500	< 3
Drawing polymer[a]	$10–80 \times 10^6$	$10–50 \times 10^3$	10–50	1–10
Graphite–epoxy laminate[b]	$\sim 1 \times 10^6$	100×10^3	$< 10^3$	< 3
Graphite–epoxy three-dimensional weave[c]	$\sim 1 \times 10^7$	$\sim 1 \times 10^6$	$\sim 10^3$	~ 100
Ceramic	0	1	10^3	10^{-6}
Fibrous ceramic composite[d]	$\sim 1 \times 10^6$	5×10^3	10^3	< 1
Composite of chains[e]	25×10^6	–	50	–

[a] Strongly rate sensitive.
[b] From unpublished work of G. Eckold.
[c] W_p estimated from tow straightening effects.
[d] For relatively weak fibre–matrix interfaces.
[e] J_c and l_{ch} are not defined because a dominant crack never forms.

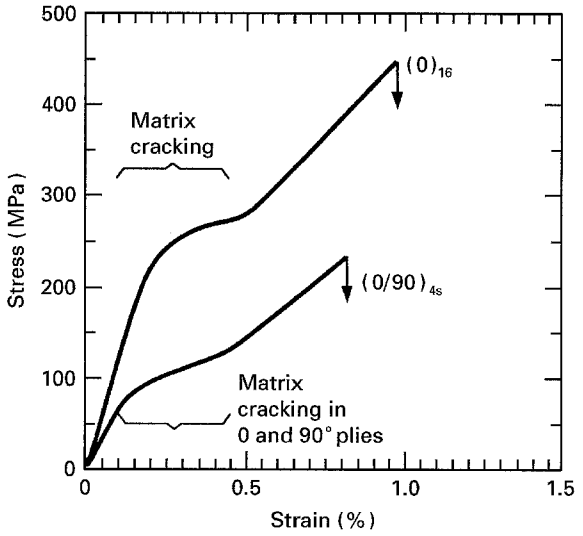

Figure 3 Stress–strain curves for typical composites of brittle fibres in a brittle matrix (SiC–glass) in uniaxial tension (taken from [5]). Data are shown for a unidirectional material and a 0/90° laminate, both loaded along the 0° direction. Both materials exhibit multiple matrix cracking, which occurs without catastrophic fibre failure because the fibre–matrix interfaces are weak.

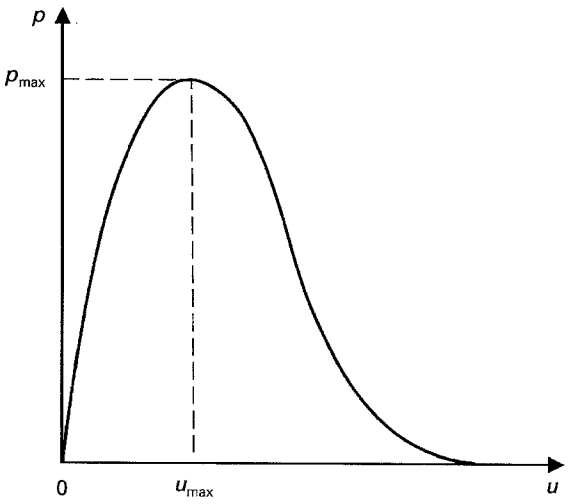

Figure 5 Typical relation $p(u)$ for a ceramic matrix composite in which bridging fibres break and pull out in the wake of a matrix crack.

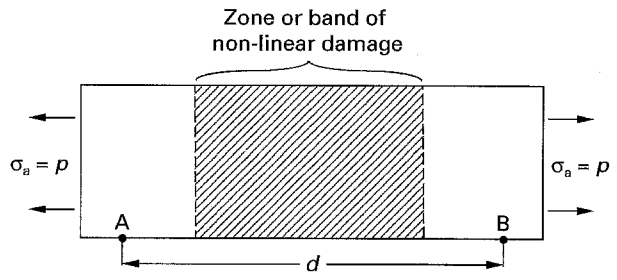

Figure 4 The relation between the bridging tractions, p, and the crack opening, u, can be inferred from a tensile test if damage is confined to a band within the gauge section. The opening displacement, u, is half the displacement discontinuity that arises across the damage band when the elastic displacement has been subtracted out. The tractions, p, are simply the uniform applied stress. Textile composites admit this simple test because the characteristic length, l_{ch}, is so large: it is always easy to create a damage band with essentially uniform tractions across it in a specimen of width $< l_{ch}$.

is no global plasticity during the formation and rupture of the band, then whatever the mechanisms underlying $p(u)$ and whatever the shape of $p(u)$, the work of fracture, W_F, is just [11–13]

$$W_F = 2\int_0^{u_{max}} p(u)\mathrm{d}u \tag{4}$$

where $p(u) = 0$ when $u \geqslant u_{max}$. (For a matrix crack in a composite, distinct mechanisms often govern the advance of the crack tip through the matrix and the bridging tractions. In this case, W_F should have added to it the intrinsic work of fracture of the matrix itself [14]. This contribution is unimportant here.)

The work of fracture is usually measured in notched specimens whose dimensions satisfy the conditions of small scale yielding or small scale bridging (e.g. [13]). However, sometimes it can be inferred directly from uniaxial tension tests of unnotched specimens. Over scales much larger than the fibre diameter, fibre rupture and pull-out occur in fibrous brittle matrix composites uniformly across a tensile specimen and independently of specimen width (Fig. 1c). Most of the work of fracture, which comes from fibre pull-out

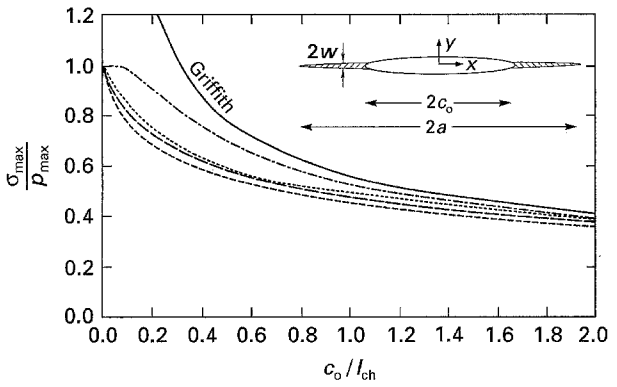

Figure 6 Notched strength when all material non-linearity (damage) is confined to a narrow, localized band (inset). The curves show strength in the limit $a \to \infty$. The universal role of the length scale, l_{ch}, is demonstrated by the asymptotic coincidence of curves for materials with very different constitutive laws obtaining in the damage band (from [17]). References to the original publications of separate curves are: (·—·) rectilinear [16], (– – –) linear softening [17], and (————) square root [21]. The curve for linear hardening (—·—) has been reproduced from [22], to repair numerical inaccuracy in [17].

following rupture, is then given directly by equating the applied load to p and deducing the opening displacement $2u$ via Equation 2 (see also Fig. 4). In this analysis, the global strain, ε, in Equation 2 must be the average strain in the composite with multiple matrix cracks (far from the damage band) during unloading, which is dictated by the mechanics of reverse fibre sliding [4, 15].

1.4. Notch sensitivity of ultimate strength

Once a localized damage band has formed, the dependence of ultimate strength, σ_c, on notch size, c, is determined entirely by the bridging law $p(u)$. Energy arguments suggest [16, 17] that notched strength for different $p(u)$ should fall near a universal curve when σ_c is normalized against p_{max}, the maximum value of p, and c is normalized by the length scale

$$l_{ch} = \frac{E' W_F}{p_{max}^2} \tag{5}$$

where E' is an elastic constant (dimensions of stress) given for orthotropic materials in [18]. The length scale, l_{ch}, is approximately the characteristic size of the equilibrium bridging zone, i.e. the zone size when the crack satisfies the small scale bridging condition and the ligaments at the rear of the bridging zone are in the process of failing [16, 19, 20]. Fig. 6 (after [17]) compares notched strength curves for four important bridging laws: uniform p (Dugdale zone), linear tension softening, linear hardening, and a quadratic law $p \propto u^{1/2}$ (as for sliding fibres constrained by friction [23]). The curves in Fig. 6 were computed by determining the applied load, σ_c, required to cause complete bridging ligament failure ($p = 0$) at the notch root for a damage band of infinite extent. For damage bands of finite extent, higher values of σ_c would be found (e.g. [13, 24]). However, in the materials of most interest here, the resistance to propagation of the damage band is weak, so that propagation to long bands generally precedes ligament failure at the notch root; and Fig. 6 is a useful guide to notched strength. When $c \gg l_{ch}$, all four curves in Fig. 6 converge to a common curve corresponding to an equivalent Griffith crack (bridging zone of length zero), which propagates when the crack tip stress intensity factor, K_{tip}, satisfies

$$K_{tip}^2 / E' = W_F \tag{6}$$

with W_F given by Equation 3. Thus for $c \gg l_{ch}$, the material is notch sensitive: $\sigma_c \propto c^{-1/2}$. When $c < l_{ch}$, the strength remains bounded by p_c, because, for a crack that is already long, the bridging ligaments are the only load bearing material in the damage band. For $c < l_{ch}$, the details of notch sensitivity depend strongly on the shape of $p(u)$. For example, as $c \to 0$, $\sigma_c \to p_c$ for the Dugdale zone, while $1-\sigma_c \propto c^{2/3}$ when $p \propto u^{1/2}$ [21], and $1-\sigma_c \propto c^{1/2}$ for linear hardening $p(u)$ [22].

2. Damage delocalization in three-dimensional woven graphite–epoxy composites

Several papers have appeared recently on failure mechanisms in three-dimensional woven graphite–epoxy composites [25–28]. These materials are exemplified by Fig. 7. They consist of two sets of nominally straight tows, namely stuffers and fillers, which form a 0/90° array; and a relatively low volume fraction of interlock tows (warp weavers), which provide continuous reinforcement in the through-thickness direction. Further details of reinforcement patterns in typical three-dimensional weaves appear in [25, 26, 29].

Along with other remarkable properties in compression, following impact, and in fatigue, three-dimensional woven composites exhibit unusually high toughness in tension. Fig. 8a shows a typical stress–displacement curve obtained with a dog-bone specimen loaded uniaxially along the stuffer direction; while Fig. 8b shows the condition of the gauge section late in the experiment. Failure in tension occurs by the rupture of individual stuffers followed by stuffer pull-out. Tow pull-out lengths are very large, commonly $\sim$10 mm, partly because of the large diameter of individual tows ($\sim$1 mm) [26]. But pull-out lengths are also influenced by the distribution of flaws. In three-dimensional composites, the main flaws are geometrical distortions created during manufacture, which are generally pronounced and broadly distributed in space [25, 26].

Fig. 8a indicates substantial non-linearity prior to the sharp load drop. This part of the data is quite unusual. The load drop occurs at a strain typically in the range 2.5–4%, which is well above the strain to failure of similar fibres and resin in unidirectional tape laminates ($\approx$1.5%)*. Some of the additional strain to peak load arises from the straightening of waves and

*See data compiled by N. Johnson and C. C. Poe, NASA Langley Research Center, Hampton, Virginia [28].

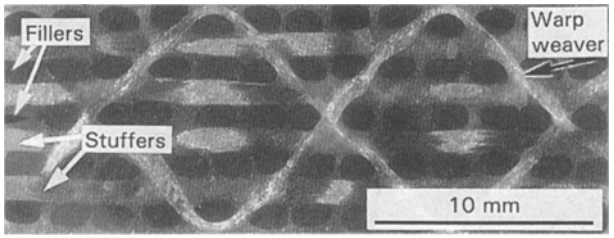

Figure 7 Section of a through-the-thickness angle interlock graphite–epoxy three-dimensional woven composite (from [25]).

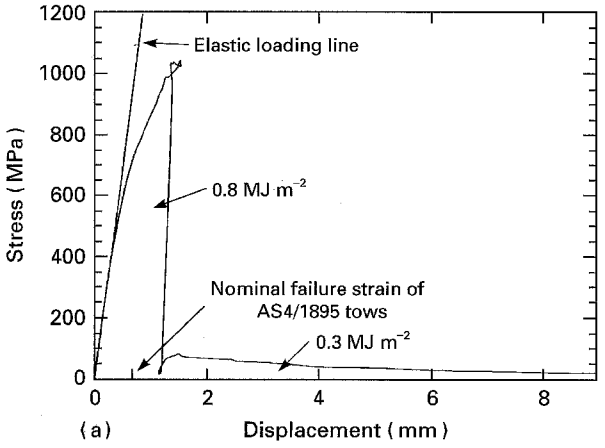

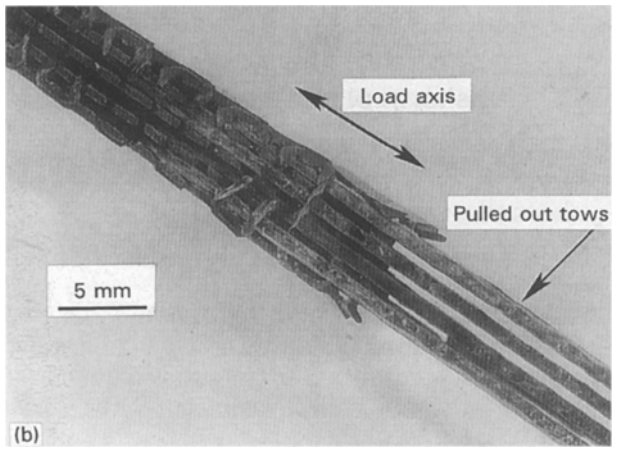

Figure 8 (a) Load–displacement record for a typical displacement control, uniaxial tension test of a three-dimensional interlock woven composite of AS4 graphite tows in Shell 1895 epoxy resin. The displacement is that of one end of the gauge section relative to the other. A displacement of 2 mm corresponds to an average engineering strain of 4.5%. The displacement beyond that expected for linear elasticity can be used to estimate the work of fracture. Estimated contributions from the two parts of the curve are shown. The total aligned fibre volume fraction was ~ 35% in this material (from [28]). (b) Extensive tow pull-out following tensile failure.

crimp irregularities in the stuffers. Irregularities in nominally straight tows are always present in current textile composites [25, 26]. However, available measurements of tow irregularity imply maximum strains of 0.25% from this source in the composite of Fig. 8a [28]. Non-linearity at strains exceeding 1.8% and up to the strain to peak load ($\approx$3.3%) is associated with tow rupture. Indeed, all stuffers (aligned tows) have failed well before the sharp drop in the applied load has been reached [28]. Thus the specimen possesses some mechanism for transferring load around sites of tow failure while the far field load holds steady near its peak value or in some cases continues to rise.

Such load transfer is believed to occur via a lock-up mechanism involving tow waviness [28]. Crimp features are found damaged but not entirely straightened on pulled-out tows following tensile failure, implying that they have been dragged through the composite during pull-out in their crimped condition. Lock-up could occur during the pull-out process when crimp asperities on adjacent tows come into contact. The contact forces in three-dimensional composites can be especially high because the through-thickness reinforcement prevents contacting tows from separating to facilitate sliding.

Like a fibrous ceramic matrix composite, and unlike a ductile metal or polymer, the three-dimensional woven composites show only small lateral contractions during extension: the material volume increases as gaps appear, especially between transverse tows. Thus, there is no significant distinction between engineering and true stress during the tensile test for strains beyond 1%. Furthermore, the damage shown in Fig. 8b is uniform across the width of the specimen, apart from statistical fluctuations in pull-out lengths. Therefore, Fig. 8a is a direct guide to the relation $p(u)$: p can be identified with the applied load and u can be deduced from the total displacement via Equation 3. When the resulting function is substituted into Equation 4, the work of fracture is estimated to exceed 1 MJ m^{-2}. The majority of this work derives from non-linearity prior to peak load; and the greater part of this arises from lock-up effects, the lesser part from plastic tow straightening [28]. The contribution from extended pull-out at low, post-peak loads is substantial but smaller (Fig. 8a).

3. Composites of chains

The action of distributed flaws and lock-up mechanisms can be further illustrated by model composites. Consider, for example, the composite of carbon steel chains illustrated in Fig. 9. Each chain is embedded in the collapsed condition shown, so that it must be stretched out before one link transfers load directly to the next. A composite is formed by embedding the chains in a polymer matrix. (The environmentally concerned might prefer to try a matrix of ice; John Webster, private communication). Since the matrix is weak, it will fail or deform before individual links of the chain fail. The chains occupy approximately 15% of the volume of the composite.

Failure under tensile loading proceeds as follows. Non-linearity begins via microcracking and local deformation of the matrix, including damage at site A of Fig. 9. This permits movement of two interlocked links towards a position where load is transferred directly from one to the other. When the links approach contact, the local material stiffness rises, preventing further local deformation. This is a lock-up mechanism. Since the links are relatively strong, subsequent damage must occur in the matrix at some other location.

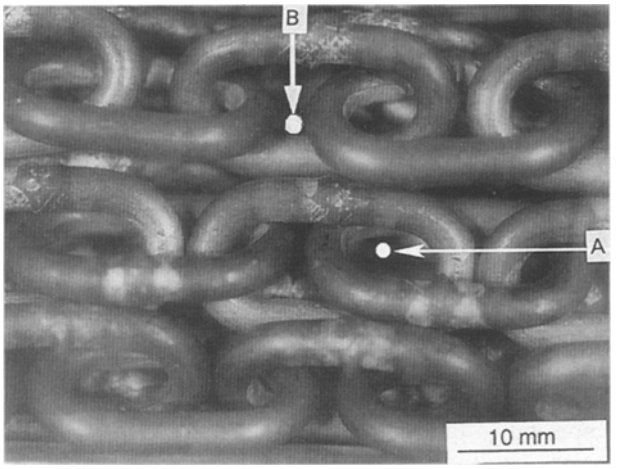

Figure 9 A composite of common carbon steel chains in an epoxy resin. Note that the chains have been laid up in a contracted configuration, so that a strain of ~30% is required to draw them taut. The resin in this picture is transparent.

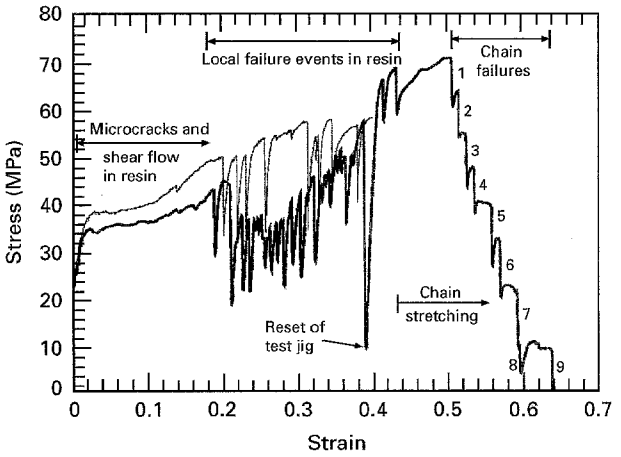

Figure 10 Engineering stress–strain curves for model composites of chains in resin; heavy curve without lateral constraints, fine curve with lateral constraint over part of the gauge section.

By repetition of this sequence, damage occurs to the matrix over the entire composite before links begin to fail.

A typical engineering stress–strain record and the prevailing mechanisms in each strain domain are shown in Fig. 10. (The composite of chains develops even less lateral contraction than the three-dimensional woven composites during the tensile test: the material volume increases as large gaps appear between resin fragments. Thus, as for fibrous ceramic matrix composites and three-dimensional woven composites, the engineering stress and the true stress, defined as average tractions over surfaces bearing many cracks, are essentially the same.) Until strains exceed 0.4, the individual chain links exhibit negligible plastic deformation. At higher strains, they narrow and stretch. Finally, each chain in the specimen fails, with the failure occurring at different strains because of random differences in the way in which they were laid down in the contracted configuration. The specimen of Fig. 10 contained nine chains in all, each of which caused a pronounced load drop when it failed.

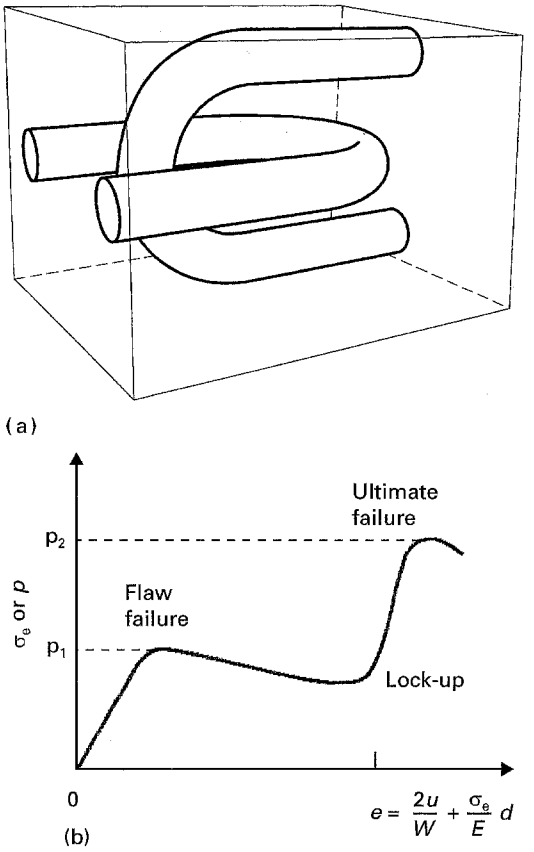

Figure 11 Schematics of (a) a representative volume element in the composite of chains, and (b) the constitutive properties of the element.

At the point of first chain failure, the damage in the composite of chains is uniformly distributed when viewed over gauge lengths much greater than the link length. Damage has extended over the entire specimen without the formation of a localized damage band. The relevant energy associated with the damage is therefore the plastic work per unit volume, W_p. It can be found by integrating Fig. 10, terminating the integral at strain, $\varepsilon = 0.4$, to avoid any contribution from plastic deformation of the chain links. This yields $W_p \approx 25\ \mathrm{MJ\,m^{-3}}$, which is at least an order of magnitude higher than values for continuous fibre brittle matrix composites (Table I). It is also much higher than values for 0/90° graphite–epoxy laminates. It is comparable to the global plastic work expended in failing ductile metals or polymers.

The processes of matrix cracking, link displacement and lock-up involving a single pair of interpenetrating links can be considered to occur inside a representative volume element of the composite (Fig. 11a). The stress–strain constitutive law for this element is shown schematically in Fig. 11b. After a brief initial elastic segment, a relatively large displacement or averaged strain occurs as the links displace towards one another. The displacement involves a complicated system of microcracks, which dissipate significant energy in creating new fracture surfaces and in friction. Fig. 10 suggests that the stress during this phase is comparable to that required to initiate non-linearity (p_1 in Fig. 11b). The stress in the representative volume element increases as the links approach one another and high compressive stresses arise in the resin

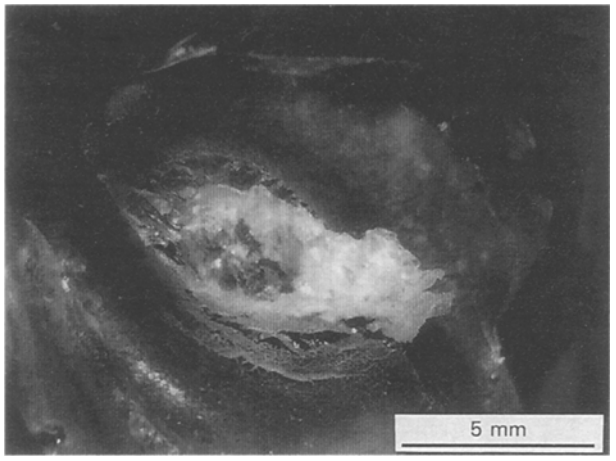

Figure 12 Fragment of epoxy that had been entrapped between two interpenetrating links. The beds once occupied by the links are the smooth, curved surfaces at top and bottom. The whitish central area is a fracture surface formed under hydrostatic compression.

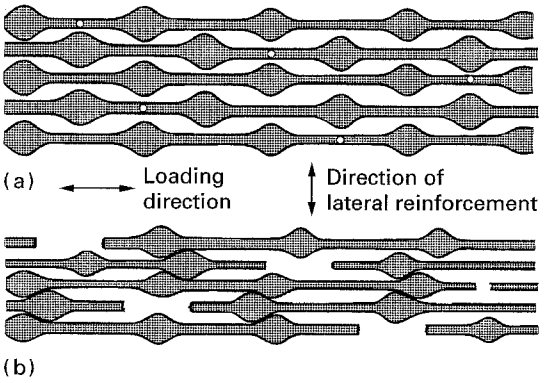

Figure 13 (a) Tows (or other reinforcing elements) bearing asperities, represented schematically. Lateral separation is inhibited by reinforcement (not drawn) in the through-thickness (vertical) direction; e.g. by warp weavers in a three-dimensional interlock weave. Designed flaws are marked by open circles. (b) The formation of unbroken load paths by the lock-up of asperities following tow failures at each of the designed flaws.

entrapped between them. Like many brittle materials, this highly constrained, compressed piece of epoxy absorbs considerable energy before it fails. When it finally does, the resulting epoxy fragments depart from the specimen with considerable velocity and there is a distinct load drop in the composite; the many spikes between strains of 0.2 and 0.4 in Fig. 10. Fig. 12 shows one such fragment. The whitish central area displays a high energy local fracture, quite distinct from the brittle crack fracture surfaces observed on all other microcracks in the epoxy. The representative volume element suffers ultimate failure only when a link fails at stress p_2.

The composites of chains do not exhibit cold drawing, i.e. the formation and self-similar propagation of a neck, as in a cold-drawing polymer. Instead, damage occurs randomly but uniformly throughout the specimen. Necking instability is pre-empted by the weak coupling of adjacent chains and the absence of geometrical stress enhancement due to lateral contraction. In terms of the constitutive properties of the representative volume element (Fig. 11b), delocalization simply requires $p_2 > p_1$. Fig. 10 suggests $p_2 \approx 1.3p_1$. (The stress within the metal of a single link when if fails is much greater than p_1. But the metal phase constitutes only a small volume fraction of the composite and therefore the representative volume element).

The average stress required to strain the composite to the point where all links are in contact can be increased by confining the specimen in a sheath. This inhibits the loss of epoxy fragments and forces links to work their way through more material. Confinement was effected crudely in one test by clamping metal plates around the gauge section. Of course, as the specimen lengthened during testing from an initial gauge length of ~ 0.12 to ~ 0.17 m at a strain of 0.4, it was no longer wholly covered by the plates and many resin fragments were still lost. Nevertheless, fragments were held in place in the confined volume and there was a substantial increase in stress over the strain interval [0.2, 0.4] (see the fine curve data of Fig. 10). (The variation in stress from specimen to specimen is less than the difference seen between the two curves of Fig. 10. The stress–strain curves for different specimens are surprisingly consistent, given the loose control exercised over chain positioning during fabrication.)

4. Damage delocalization in a composite of brittle constituents

To achieve damage delocalization and high levels of plastic work in a brittle–brittle composite, three conditions must be satisfied

1. Flaws must be distributed throughout the material.
2. Localized failure at a flaw must be followed by significant local displacements to accommodate the absorption of plastic work.
3. Lock-up must raise the strength of locally failed material to levels exceeding the stress required to initiate damage at other flaws: i.e. in the schematic of Fig. 11b, $p_2 > p_1$.

These three conditions are obviously met in the composite of chains. The flaws are no more than regions of resin that are exposed to unusually high stress by their position relative to chain links; for example, the resin between alternative links in the same chain (point B in Fig. 9). The lock-up mechanism is so strong that resin failure occurs both at such sites and elsewhere all over the specimen before the stress, p_2, is exceeded anywhere. The shape (aspect ratio) of the links ensures that large strains are attained in representative volume elements before lock-up, which favours high energy absorption.

Whether it is practicable to fabricate chain composites with advanced materials (carbon, ceramics, etc.) is rather doubtful. The topology of interpenetrating links presents a challenging processing problem. A more viable approach may be via textile composites like those of Fig 7. Fig. 13 shows a schematic generalization of the salient internal

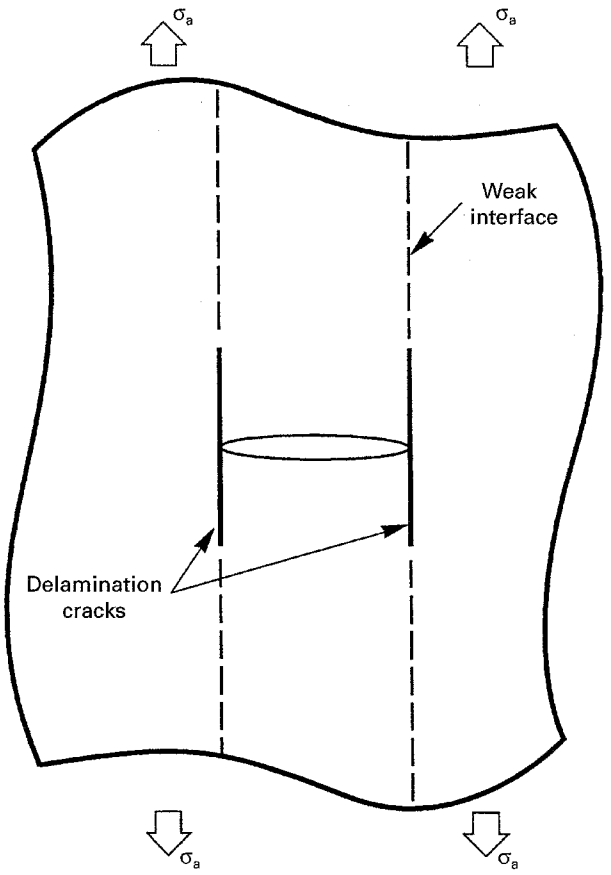

Figure 14 Possible decoupling of a notch from surrounding material by delamination cracks.

geometry of such composites. Reinforcing elements (which may be fibre tows, solid rods, or even laminae) contains asperities and designed flaws of strength p_1. Fig. 13a shows one spatial distribution of designed flaws that could lead to delocalized damage. Not all intervals demarked by asperities contain flaws. Thus, even when all designed flaws have failed, continuous load paths are restored through undamaged reinforcing elements following sliding displacement of broken reinforcing elements and lock-up via asperity contact. In terms of a representative volume element analogous to that in Fig. 11, subsequent damage, either at contacting asperities or in unfailed sections of reinforcement, must occur at some characteristic local stress, p_2. If tensile strains do not generate lateral contractions, p_1 and p_2, which are *volume averages* rather than stresses in surviving ligaments of material, can be regarded as engineering stresses. Then, for delocalization to be possible, $p_1 > p_2$.

The composite of chains and the schematic of Fig. 13 share an important characteristic. Lock-up is achieved by arranging the geometry of the reinforcement in such a way that local failure under remote tension leads to the development of large compressive local stresses. It is hard to conceive of a mechanism for high global plastic work in a brittle–brittle composite that does not rely on generating local compression. Brittle materials are strong in compression, even in states of high damage.

5. Strength and stiffness

When flaws are introduced into a material to achieve delocalization, strength must be sacrificed. However, the loss of strength need not be large. In a brittle–brittle composite, yield strength will be determined by the flaw strength; i.e. p_1. For unnotched specimens, the only requirement on p_1 is the inequality $p_1 < p_2$. (See Section 6 for the strong effect of notches.) However, both p_1 and p_2 will usually be random variables, with some characteristic distributions. How far apart the average values of p_1 and p_2 must be kept will depend on the widths of their distributions, which will depend on the degree of control possible in processing.

Ultimate strength depends on the spatial density of flaws (and thus local damage events) and the lock-up mechanism. In a system like that illustrated in Fig. 13, ultimate strength is determined by the partitioning of stress among intact segments of reinforcement after all flaws have failed and lock-up has been achieved in all representative volume elements. This difficult question will be resolved only after considerable research.

In the schematic of Fig. 13, the presence of designed flaws need have no major effect on stiffness, at least until local failures trigger the large displacements that precede lock-up. Following lock-up, composite stiffness can again be close to that expected for pristine reinforcement.

In the composite of chains, composite stiffness in the contracted configuration can be estimated by regarding the chain links as discontinuous reinforcing rods of modulus, E_f, in a relatively soft matrix (shear modulus, G_r). Load is transferred from one link to another largely by shear stresses in the resin. Since the resin is relatively compliant, the maximum composite stiffness that could possibly be achieved is approximately fE_f, where f is the volume fraction constituted by the chains. This limit can be approached only if the links are very long compared to the characteristic length, l, set by shear load transfer

$$l \sim D(E_f/G_r)^{1/2} \tag{7}$$

where D is the link diameter. This condition is not satisfied by the composites of chains tested here; their moduli ($\approx$8 GPa) are therefore much lower than $fE_f \approx 30$ GPa ($f \approx 0.15$; $E_f \approx 200$ GPa for carbon steel).

6. The effect of a notch on delocalization

Consider a sharply notched specimen of a material whose constitutive properties are similar to those of Fig. 11b: a material in which any local failure event at stress p_1 is followed by lock-up and ultimate failure at a higher stress, p_2. In general, damage can emanate from the notch in a zone of any shape. Calculating the stress distribution, the shape of the damage zone, and whether damage will be localized or delocalized is not an analytically tractable problem. Numerical solutions are required. Nevertheless, qualitative insight into the localization–delocalization transition can be gained by *assuming* that the damage develops along a narrow band as in the inset in Fig. 6. The non-

linearity within the damage band can be represented by a cohesive or bridging zone, in the usual way. The constitutive behaviour of the band is summarized by the relation $p(u)$ between the stress across the band and the displacement discontinuity, $2u$, it introduces into the elastic body. For damage that is uniformly distributed from top to bottom of the band (but with no assumption made about its distribution along the band), one has

$$p(u) = \eta\sigma(u/w) \tag{8}$$

where the dimensionless factor, η, is unity in the absence of lateral contractions; $\sigma(\varepsilon)$ is the constitutive relation of Fig. 11b; and $2w(x)$ is the width of the band, a function of the position variable x (Fig. 6). (More generally, Equation 8 should involve an integral of damage distribution over $-d < y < d$ whose value will depend on the spatial distribution of the flaws of strength p_1 and the mechanisms for relieving stress concentration around failed flaws, among other things. However, this factor may be assumed ~ 1 without vitiating qualitative arguments.)

The condition for damage to be delocalized is that the far field stress should exceed p_1 *before* the ligament of damaged material at the notch root reaches the stress p_2. If it does not, then catastrophic failure will commence at the notch root while the material in the far field is as yet undamaged. When damage is confined to a narrow band with a bridging constitutive law like Equation 8, then the required information is immediately available from the notched strength curves of Fig. 6. Identifying σ_c and p_{max} of Fig. 6 with p_1 and p_2, respectively, Fig. 6 becomes a plot of the maximum ratio, p_1/p_2, that can be tolerated to avoid catastrophic failure, i.e. to achieve delocalization, versus the notch size. Or, alternatively, for a given notch size, Fig. 6 shows the reciprocal of the minimum ratio, p_2/p_1, required to ensure delocalization. (Here, of course, p_1 and p_2 are being considered deterministic rather than random variables.)

The effect of a notch is very strong. For all cases in Fig. 6 except Dugdale's law p = constant, the critical maximum ratio, p_1/p_2, falls very rapidly from the value unity for a notch free specimen*. Notch insensitivity of the localization–delocalization transition is favoured by mechanisms leading to $p \approx$ constant initially, followed by hardening to the ultimate strength, p_2.

Alternatively, notch insensitivity of a material's propensity for delocalization can be promoted by providing a mechanism for easy shear failure, e.g. weak interfaces lying in the loading direction and normal to the notch. If the work of fracture of such interfaces is one-eighth [30] or one-quarter [31] that for a mode I crack propagating from the notch, then the latter will not occur. Instead, delamination or splitting interface cracks will divide the specimen into non-interacting notched and unnotched strips (Fig. 12). Delocalization in the unnotched strips will be unaffected by the original notch.

Decoupling notches by delamination will probably always be much more easily achieved as a method of averting damage localization in composites than arranging that $p \approx$ constant in the presence of mode I damage zones.

7. Optimizing work of fracture

If it is given that damage localization will occur, the same geometry-induced mechanisms that might have favoured delocalization will tend to enhance the work of fracture, W_F. For damage localization in a band, Equation 4 applies: the area under the curve $p(u)$ is to be maximized. Distributed flaws, large local displacements following flaw failure, and local hardening via lock-up prior to ultimate failure are all favourable. There will usually be much more work in a constitutive law like Fig. 11b than in one like Fig. 5, which is typical of current continuous fibre ceramic matrix composites. Optimizing W_F and striving to achieve delocalized damage will evoke similar concepts for internal composite geometry.

8. Non-optimality of current composites

By virtue of their internal geometry, both textile composites and the composite of chains show exceptional properties. Textile composites possess a work of fracture that surpasses that of any other group of engineering materials. The composite of chains absorbs global plastic work that rivals that of ductile materials, even when its constituents are behaving as brittle materials. Yet neither textile composites nor the composite of chains have been optimized. On the contrary, the work of fracture of the three-dimensional woven composites has been achieved by pure accident. Interlock weaves have been fabricated to date without any regard to mechanical properties beyond the elasticity and ultimate strength implied by rules of mixtures. Any lock-up effects are an unintended consequence of geometrical irregularity, which has resulted from the difficulty of controlling the weaving process [26, 28]. As for the composite of chains, it was cooked up with whatever carbon steel chains could be bought in 48 h for less than a dollar a foot; and whatever spare resin lay in the laboratory. With high aspect ratio links to maximize local displacements prior to lock-up (and initial stiffness), a stronger, brittle matrix, and some mechanisms for avoiding the loss of matrix fragments during failure, the global plastic work, W_p, could surely exceed the highest values recorded for ductile metals or polymers.

*The reader can confirm the strong effect of a notch on the cold drawing of polycarbonate by a simple experiment. Cut a dog-bone specimen about 20 × 100 mm from a polycarbonate sheet, e.g. a zip-lock bag. Load in tension with thumbs and fingers. If the sides of the specimen have been smoothly cut and the load rate is not too high, cold drawing is easily achieved. Now repeat the experiment after making a nick of <1 mm on one side of the specimen with a razor blade. The specimen will now show localized failure. The minimum nick to achieve this transition is very small. The ratio p_1/p_2 for polycarbonate is not much less than one, as suggested by the flatness of the engineering stress–strain curve in Fig. 2a during cold drawing.

9. Wood and other systems of off-axis fibres

Composites whose internal geometry lends them favourable fracture properties have long since evolved in nature. In wood, microfibrils of cellulose are arranged in cell walls in approximately helical paths, inclined to the grain at all angles, but with the majority between 10 and 30° [32]. Thus, in combination with the hemicellulose and lignin which bind them together, the cellulose microfibrils form highly anisotropic composite shells within the cell walls, with far greater stiffness parallel to the microfibrils than perpendicular to them and relatively low axial shear stiffness, much like manmade, filament wound composite shells. Under tensile loads parallel to the grain, the cellulose microfibrils tend to straighten out, tearing apart at high strains. Such cell wall splitting causes extensive deflections of the macroscopic tensile crack, with energy absorbed both by the splitting process itself and frictional pull-out effects [33].

It has also been suggested that the asymmetric helical winding of cell walls can cause tensile buckling, a reversible elastic instability [34–36]. The buckling may involve strains for some individual cells as high as 20% and high rates of energy absorption even in the absence of plastic tearing. However, the more commonly held view is that irreversible damage to cell walls is the primary contributor to the work of fracture.

In all, wood is very tough, at least for loading along the grain. The specific work of fracture of wood rivals that of any other group of materials [33, 37]. However, the system of cells does not harden overall during the damage process and wood does not exhibit significant global plasticity. There is apparently no natural selection process favouring delocalized damage or cold drawing amongst trees.

The energy absorbing qualities of helically wound fibres have also been exploited in synthetic composites. Assemblies of hollow, wound cylinders possess work of fracture values between 200 and 500 $kJ\,m^{-2}$, somewhat higher than more common engineering materials [36]. Within the fatal damage band, the total plastic work per unit volume is $\sim 10\,MJ\,m^{-3}$, distributed over a damage band, i.e. a band of tensile buckling and tearing, approximately 30 mm wide [36]. However, like wood, these wound composites apparently did not exhibit significant global damage over long gauge lengths.

The benefits of off-axis fibres can only be expected in anisotropic composites. In a brittle–brittle composite, the fibre and the matrix often have very similar, approximately isotropic, elastic properties. In this case, there is no advantage in winding the fibres. The fibres will fail before they straighten very far (unless the matrix is very weak and porous); there can be no tensile buckling; nor will fibre straightening cause hardening.

In materials that are highly anisotropic, such as fibre reinforced polymers, significant global damage can be achieved by fibre straightening provided the fibres are predominantly off-axis. Recent examples have been demonstrated with flat braided panels and braided tubes [38, 39]. However, in these cases plasticity is bought at a severe price in stiffness and strength, because of the absence of significant numbers of axial fibres. When axial fibres are added, global plasticity is minimal and failure reverts to a catastrophic localized band.

10. Scales

The characteristic material lengths, l_{ch}, which plays a fundamental role in determining notch sensitivity of both strength and the localization–delocalization transition, is not directly related to any length scale possessed by the microstructure or internal composite geometry. It derives simply from the work of fracture, the maximum bridging traction, and the composite modulus (Equation 5). Materials whose internal structure involves multiple length scales often have high work of fracture, because their fracture surfaces tend to have high fractal dimension. Wood, seashells, tendons and bones are naturally occurring examples. In as much as multiple length scales augment W_F, they will favour notch insensitivity and damage delocalization by increasing l_{ch}.

Yet multiple length scales are not a *necessary* design goal. High values of l_{ch}, notch insensitivity and the delocalization of damage can be achieved in a composite whose internal geometry has a single characteristic length e.g. the link size in the composite of chains. Neither is there necessarily a direct relationship between the magnitude of the single length scale and composite properties. In the composite of chains and perhaps in the three-dimensional woven composites, the constitutive properties (and hence W_F, l_{ch} and the propensity for delocalization) depend primarily on *mechanisms* of damage (flaw populations, local displacements and lock-up) that are governed by the geometrical shape of the reinforcement; its scale may be secondary.

Thus the mechanisms of toughening highlighted here, namely localized failures, local displacement and particularly lock-up, are distinct from the effects of hierarchical spatial scales.

11. Conclusions

Internal geometry can have a profound effect on the nature of damage evolution in composites. Damage delocalization and, if localization occurs, fracture toughness are both favoured by building a combination of flaws and lock-up mechanisms into a material. In brittle–brittle composites, tailoring internal geometry to convert far-field tension into local compression appears to be the most promising method for achieving levels of global plastic work and work of fracture that rival ductile engineering materials.

Acknowledgements

The author's proclivity for oversimplifying and ignoring precedent was blunted to some extent and always in a very agreeable way by Drs Mike Ashby, Brian

Derby, David Marshall, Zhigang Suo and Cedric Turner. Mr R. V. Inman fabricated the composites of chains and Mr Jonathan Flintoff performed the tests of Fig. 10, both very professionally. All work was funded by Rockwell Independent Research and Development.

References

1. M. R. PIGGOTT, "Load Bearing Fibre Composites" (Pergamon, Oxford, 1980).
2. W. JOHNSON and P. B. MELLOR, "Engineering Plasticity", (Van Nostrand Reinhold, London, 1973).
3. I. M. WARD, "Mechanical Properties of Solid Polymers". (Wiley Interscience, London, 1971).
4. J. AVESTON, G. A. COOPER and A. KELLY, in "The Properties of Fiber Composites, Conference Proceedings", National Physical Laboratory, (IPC Science and Technology Press, Guildford, 1971) pp. 15–24.
5. D. S. BEYERLE, S. M. SPEARING and A. G. EVANS, *J. Amer. Ceram. Soc.* **75** (1992) 3321.
6. L. N. McCARTNEY, *Composites* **24**, (1993) 84.
7. D. S. DUGDALE, *J. Mech. Phys. Solids* **8** (1960) 100.
8. R. M. L. FOOTE, Y.-W. MAI and B. COTTEREL, *ibid.* **34** (1986) 593.
9. M. ELICES and J. PLANAS, in "Fracture Mechanics of Concrete Structures," edited by L. Elfgren (Chapman and Hall, London, 1989) Chap. 3.
10. E. PASSAGLIA, *Polymer* **25** (1984) 1727.
11. L. R. F. ROSE, *J. Mech. Phys. Solids* **34** (1987) 383.
12. B. BUDIANSKY, J. W. HUTCHINSON and A. G. EVANS, *ibid.* **34** (1986) 167.
13. G. BAO and Z. SUO, *Appl. Mech. Rev.* **45** (1992) 355.
14. B. N. COX and D. B. MARSHALL, *Acta Metall. Mater.* **42** (1994) 341.
15. J. W. HUTCHINSON and H. M. JENSEN, *Mech. Mater.* **9** (1990) 139.
16. A. H. COTTRELL, "Mechanics of Fracture" *Tewksbury Symposium on Fracture (1963)*, edited by R. C. Gifkins (Engineering Faculty, University of Melbourne, 1965) pp. 1–27.
17. Z. SUO, S. HO and X. GONG, *J. Engng Mater. Technol.* **115** (1993) 319.
18. G. C. SIH, P. C. PARIS and G. R. IRWIN, *Int. J. Fract. Mech.* **1** (1965) 189.
19. J. R. RICE, in "Physics of the Earth's Interior, Proceedings of the International School of Physics, Enrico Fermi", edited by A. M. Dziewonski and E. Boschi, (North Holland, Amsterdam, 1980) pp. 555–649.
20. A. HILLERBORG, in "Fracture Mechanics of Concrete," edited by F. H. Wittman (Elsevier, Amsterdam, 1983) pp. 223–249.
21. B. BUDIANSKY and Y.-L. CUI, *J. Mech. Phys. Solids* **42** (1994) 1.
22. B. N. COX and L. R. F. ROSE, *Mech. Mater.* in press.
23. D. B. MARSHALL, B. N. COX and A. G. EVANS, *Acta Metall. Mater.* **33** (1985) 2013.
24. D. B. MARSHALL and B. N. COX, *ibid.* **35** (1987) 2607.
25. B. N. COX, M. S. DADKHAH, R. V. INMAN and W. L. MORRIS, *ibid.* **40** (1992) 3285.
26. B. N. COX, M. S. DADKHAH, W. L. MORRIS and J. G. FLINTOFF, *ibid.* **42** (1994) 3967.
27. M. S. DADKHAH, B. N. COX and W. L. MORRIS, *Acta Metall. Mater.* in press
28. B. N. COX, M. S. DADKHAH and W. L. MORRIS, *Composites*, in press
29. T.-W. CHOU and F. KO (editors), "Textile Structural Composites", Composite Materials Series, 3 (Elsevier, Amsterdam, 1989).
30. K. KENDALL, *Proc. R. Soc. Lond. A.* **344** (1975) 287.
31. M.-Y. HE and J. W. HUTCHINSON, *Int. J. Solids Struct.* **25** (1989) 1053.
32. J. M. DINWOODIE, *J. Microscopy* **104** (1975) 3.
33. M. F. ASHBY, K. E. EASTERLING, R. HARRYSON and S. K. MAITI, *Proc. Roy, Soc. London* **A398** (1985) 261.
34. D. H. PAGE, F. EL-HOSSEINY and K. WINKLER, *Nature* **229** (1971) 252.
35. N. J. PAGANO, J. C. HALPIN and J. M. WHITNEY, *J. Compos. Mater.* **2** (1968) 154.
36. J. E. GORDON and G. JERONIMIDIS, *Phil. Trans. R. Soc. Lond.* **A294** (1980) 545.
37. M. F. ASHBY, "*Materials Selection in Mechanical Design*", (Pergamon, Oxford, 1993) Appendix C.
38. M. S. DADKHAH, J. G. FLINTOFF, T. KNIVETON and B. N. COX, *Composites* **26** (1995) 561.
39. N. A. FLECK and A.-M. HARTE, Cambridge University, private communication.

Received 27 January
and accepted 11 May 1995